Maize *Brittle stalk2* Encodes a COBRA-Like Protein Expressed in Early Organ Development But Required for Tissue Flexibility at Maturity[1][C][OA]

Anoop Sindhu[2], Tiffany Langewisch[3], Anna Olek, Dilbag S. Multani[4], Maureen C. McCann, Wilfred Vermerris, Nicholas C. Carpita, and Gurmukh Johal*

Department of Botany and Plant Pathology (A.S., A.O., N.C.C., G.J.) and Department of Biological Sciences (T.L., M.C.C.), Purdue University, West Lafayette, Indiana 47907–2054; Department of Agronomy, University of Missouri, Columbia, Missouri 65211 (D.S.M.); and University of Florida Genetics Institute and Agronomy Department, Gainesville, Florida 32610 (W.V.)

The maize (*Zea mays*) *brittle stalk2* (*bk2*) is a recessive mutant, the aerial parts of which are easily broken. The *bk2* phenotype is developmentally regulated and appears 4 weeks after planting, at about the fifth-leaf stage. Before this time, mutants are indistinguishable from wild-type siblings. Afterward, all organs of the *bk2* mutants turn brittle, even the preexisting ones, and they remain brittle throughout the life of the plant. Leaf tension assays and bend tests of the internodes show that the brittle phenotype does not result from loss of tensile strength but from loss in flexibility that causes the tissues to snap instead of bend. The *Bk2* gene was cloned by a combination of transposon tagging and a candidate gene approach and found to encode a COBRA-like protein similar to rice (*Oryza sativa*) BC1 and Arabidopsis (*Arabidopsis thaliana*) COBRA-LIKE4. The outer periphery of the stalk has fewer vascular bundles, and the sclerids underlying the epidermis possess thinner secondary walls. Relative cellulose content is not strictly correlated with the brittle phenotype. Cellulose content in mature zones of *bk2* mature stems is lowered by 40% but is about the same as wild type in developing stems. Although relative cellulose content is lowered in leaves after the onset of the brittle phenotype, total wall mass as a proportion of dry mass is either unchanged or slightly increased, indicating a compensatory increase in noncellulosic carbohydrate mass. Fourier transform infrared spectra indicated an increase in phenolic ester content in the walls of *bk2* leaves and stems. Total content of lignin is unaffected in *bk2* juvenile leaves before or after appearance of the brittle phenotype, but *bk2* mature and developing stems are markedly enriched in lignin compared to wild-type stems. Despite increased lignin in *bk2* stems, loss of staining with phloroglucinol and ultraviolet autofluorescence is observed in vascular bundles and sclerid layers. Consistent with the infrared analyses, levels of saponifiable hydroxycinnamates are elevated in *bk2* leaves and stems. As *Bk2* is highly expressed during early development, well before the onset of the brittle phenotype, we propose that *Bk2* functions in a patterning of lignin-cellulosic interactions that maintain organ flexibility rather than having a direct role in cellulose biosynthesis.

In the type II cell walls of cereals and other commelinoid monocots, cellulose microfibrils are cross-linked mostly with glucuronoarabinoxylans and mixed-linkage β-glucans, and a strong phenylpropanoid network develops after cells stop growing (Carpita, 1996). These walls are very different from the pectin-rich type I walls of dicotyledonous species (McCann and Roberts, 1991; Carpita and Gibeaut, 1993).

Although mutants in cell wall-related genes are valuable materials to address the functions of cell wall polymers and their interactions, very few cell wall mutants have been characterized for the grasses (Yong et al., 2005). Some of the first mutations whose phenotypes suggested a cell wall defect were the *brittle stalk* (*bk*) mutants of maize (*Zea mays*), synonymous with the *brittle culm* (*bc*) mutants of rice (*Oryza sativa*) and barley (*Hordeum vulgare*; Langham, 1940; Kokubo et al., 1989; Li et al., 2003). In maize, *bk2* is characterized by a brittleness of all aerial plant organs, where the tissues easily snap when bent (Langham, 1940). Curiously, the brittle phenotype only appears after about 4 weeks of growth, under field or greenhouse conditions, about the time of appearance of the fifth leaf. Before this stage, *bk2* plants are indistinguishable from their wild-type siblings, as the leaves are flexible and can be bent easily without breaking (Langham, 1940).

To understand the molecular basis of the brittle phenotype, we cloned the *Bk2* gene and characterized

[1] This work was supported by a grant from the National Science Foundation Plant Genome Research Program (to N.C.C., M.C.C., and W.V.), Purdue University start-up funds (to G.J.), and University of Florida funds to purchase a pyrolysis mass spectrometer (to W.V.).

[2] Present address: Department of Plant Pathology, Iowa State University, Ames, IA 50011.

[3] Present address: Department of Biological Sciences, University of Missouri, Columbia, MO 65211.

[4] Present address: Pioneer Hi-Bred International, P.O. Box 1000, Johnston, IA 50131.

* Corresponding author; e-mail gjohal@purdue.edu.

The author responsible for distribution of materials integral to the findings presented in this article in accordance with the policy described in the Instructions for Authors (www.plantphysiol.org) is: Gurmukh Johal (gjohal@purdue.edu).

[C] Some figures in this article are displayed in color online but in black and white in the print edition.

[OA] Open Access articles can be viewed online without a subscription.

www.plantphysiol.org/cgi/doi/10.1104/pp.107.102582

cell structure and cell wall composition in the *bk2* mutant. The *Bk2* gene is orthologous to the rice *Bc1* gene, a member of the COBRA gene family that encodes glycosylphosphatidylinositol (GPI)-anchored proteins of unknown function (Schindelman et al., 2001; Li et al., 2003; Ching et al., 2006). A mutation in the founding member of the COBRA family in Arabidopsis (*Arabidopsis thaliana*) results in severe inhibition of root elongation and the progressive radial swelling of the cortical cells away from the root tip (Hauser et al., 1995). The *cobra* mutant is defective in cellulose synthesis and microfibril orientation in roots (Schindelman et al., 2001; Roudier et al., 2005). In contrast, rice *Bc1* is expressed primarily in vascular regions of the leaves and culm, and the phenotype results in organ brittleness rather than any obvious cell deformities. As with the rice *bc1* mutants, mutations in Arabidopsis *COBRA-LIKE4* (*COBL4*), the most similar homolog of the rice *Bc1* gene (Li et al., 2003), result in plants with normal morphology but weaker stems (Brown et al., 2005). In addition, *cobl4* exhibits an irregular xylem phenotype, similar to mutants compromised in secondary wall cellulose synthesis or lignin deposition (Brown et al., 2005).

Because *cobl* mutants have decreased cellulose contents, COBL proteins are thought to be involved in cellulose synthesis or its regulation (Kokubo et al., 1991; Schindelman et al., 2001; Li, et al., 2003; Roudier et al., 2005). Also, the brittle phenotypes of *bc1* and *bk2* were determined to be a loss of mechanical strength associated with a reduction in cellulose content (Ching et al., 2006). However, this conclusion is inconsistent with the phenotype of other cellulose-deficient Arabidopsis mutants of reduced tensile strengths but which are not brittle (Turner et al., 2001). How the loss of function of COBL4, BK2, and BC1 proteins results in a brittle phenotype remains mysterious.

Consistent with the reports by Li et al. (2003) and Ching et al. (2006), we show here that decreases in the proportion of cellulose to total cell wall mass in leaves and mature stems of *bk2*. However, this was not true of the developing stem. Further, the *bk2* mutant compensates for the loss of cellulose with an increase in wall mass, mostly xylans, per total dry mass. Additional structural features, most likely related to phenolic esters, are better correlated with the brittle phenotype. We show here that the *Bk2* gene is strongly expressed during the first 2 weeks in development, but the expression is substantially lower by the time of the appearance of the brittle phenotype at the 4-week stage. In addition, after expression of the phenotype, Klason lignin content is enriched in *bk2* stems but there is a loss of phloroglucinol-positive material and UV autofluorescence in the mature vascular bundles and sclerids underlying the epidermis. In contrast to the results of Ching et al. (2006), the mechanical or flexural strengths of wild-type and *bk2* internodes, as measured by simple one-point bend tests, were indistinguishable. However, the wild-type internodes continue to bend under increasing stress, but the *bk2* internodes bent slightly under the stress and then snapped upon continued applied stress. Our observations suggest that loss of cellulose synthesis is not tightly correlated with the brittle phenotype and that lack of proper formation of a lignocellulosic interaction during a change in lignin architecture may result in the drastic loss of flexibility exhibited in the mutant. Further, the high expression of *Bk2* during early development before the onset of the brittle phenotype and its ability to establish the number and size of peripheral vascular bundles in the basal internodes indicate that *Bk2* plays a broader fundamental role in developmental patterning.

RESULTS

Phenotypic Characteristics of *bk2*

In the uniform backcross progeny that we generated, the mutant *bk2* and wild-type siblings segregated in a 1:1 ratio, indicating that the recessive *bk2* allele transmits normally through both the male and female gametophytes. In this progeny, the mutant (*bk2*/*bk2* homozygotes) and wild-type siblings (*bk2*/+ heterozygotes) were indistinguishable in all aspects of growth, development, and vigor, except that the *bk2* mutants were brittle and broke readily (Fig. 1A). All of the plant organs are brittle, including leaves, the ear,

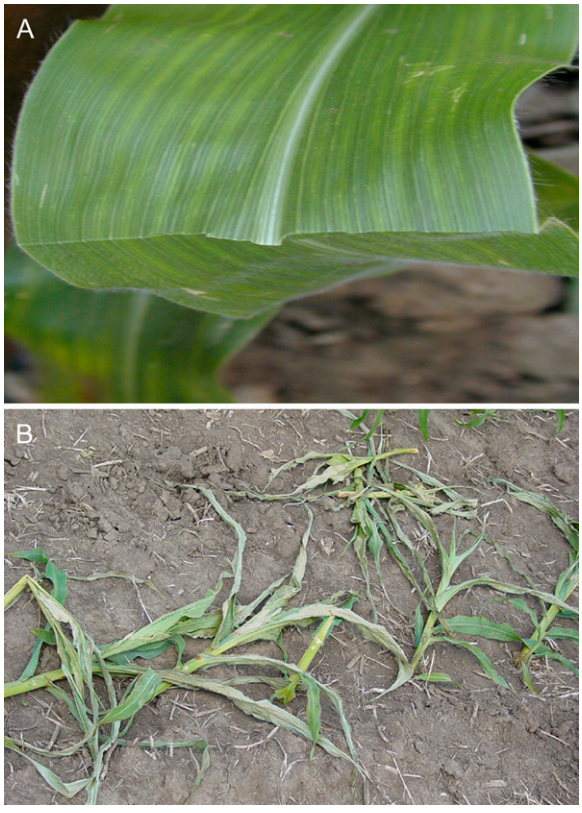

Figure 1. Characteristics of the *bk2* phenotype. A, Bending of a brittle mutant leaf causes it to snap and break cleanly, leaving razor-cut-like edges. B, Breaking of *bk2* mutants in the field as a result of wind damage. [See online article for color version of this figure.]

the tassel, and brace roots, as well as the stems. Field-grown mutants have to be staked as even a slight wind gust causes *bk2* to snap at the lower internodes (Fig. 1B).

A unique characteristic of the maize *bk2* mutant that distinguishes it from brittle mutants of other plant species is that its phenotype is developmentally programmed. During early germination and growth, the mutants are indistinguishable from wild-type siblings for the first 4 weeks after planting. Afterward, all organs of the *bk2* mutants turn brittle, even the preexisting ones, and they remain brittle throughout the life of the plant.

bk2 Mutants Exhibit Some Changes in Stem Anatomy

To determine if the brittleness of *bk2* mutants arises from changes in cell shape, size, or structure, we compared internode stem cells of *bk2* with those of their wild-type siblings using bright-field and scanning electron microscopies. Sections derived from the first, third, and fourth internodes (counted from the bottom) of the greenhouse-grown mutant and wild-type siblings were used for these comparisons.

While the wild-type stems produce secondary vascular bundles in the rind region of their lower internodes at maturity, the mutant stems do not (Fig. 2, A and B). As a result, the density of peripheral vascular bundles in *bk2* stems is only 1.7 $\pm$ 0.2 per mm compared to 3.5 $\pm$ 0.4 per mm in wild-type internodes, even though there is little difference in stem circumference. The total number of peripheral bundles was almost halved, with an average of 37 for *bk2* and 72 for wild type. The density of peripheral bundles was slightly reduced in the third internode of *bk2*, 2.4 $\pm$ 0.3 per mm versus 2.9 $\pm$ 0.2 per mm, with total peripheral bundles of 53 for *bk2* and 84 for wild type. Although most cells in the rind region had slightly thinner walls in the mutant compared to the wild type, the difference was more conspicuous in the walls of sclerenchyma underlying the epidermis and surrounding the vascular bundles (Fig. 2, C–H). Whereas the thinner *bk2* sclerenchyma walls are homogeneous in appearance, those of the wild type show separation of primary and secondary wall. There are relatively more cells in *bk2* stem cortex between the epidermis and the outer ring of vascular bundles than in those of wild type. The lowermost internodes tend to form a continuous layer of sclerids between the outermost ring of vascular bundles in wild-type plants but not in *bk2* mutants. Taken together, these observations indicate that the *bk2* mutation results in developmental alterations in the structure and anatomy of the maize stalk.

Tagging of *Bk2*

We tagged the *Bk2* gene using a directed mutagenesis approach involving *Mutator* (*Mu*; Multani et al., 2003). *Mu*-active plants were used as females and fertilized with pollen collected from the *bk2* tester homozygous for the original mutant allele, herein

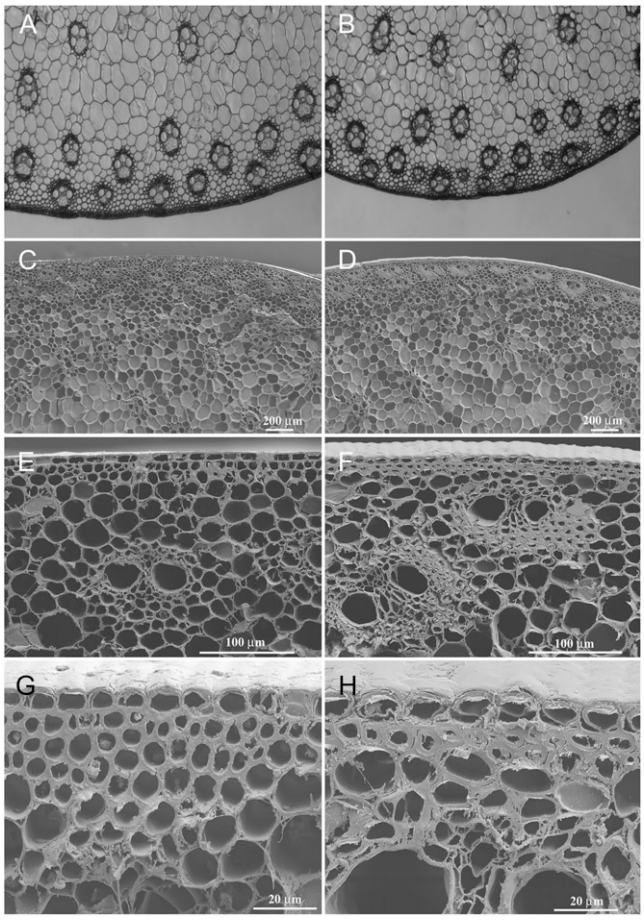

Figure 2. Anatomy of a *bk2* stalk. A and B are cross sections of the corresponding mutant and wild-type stems, respectively, imaged with bright-field microscopy. C to H, Scanning electron micrographs of mutant (C, E, and G) and wild-type (D, F, and H) stems taken from cross sections.

referred to as the reference allele (*bk2-ref*). About 60,000 of the resulting progeny were planted in the field and screened for *bk2* mutants around week 7 after planting. Brittle mutants were screened by taking a leaf from each of the progeny plants between the index and the middle finger and then bending with the thumb. Two brittle mutants were identified, but only one could be propagated. Sixteen plants from the progeny of this mutant (named *bk2-Mu1*) with B73 were genotyped using two RFLP markers, *BNL8.17*, which we found to be located 4.0 cM proximal to the *bk2* locus, and *UMC95*, which is located 2.5 cM distal to *bk2*. This analysis allowed us to identify plants that inherited the newly generated mutant allele, *bk2-Mu1*. These *bk2-Mu1* heterozygotes were crossed again to the *bk2* tester (*bk2-ref*) to generate progeny that segregated 1:1 for brittle and wild-type plants containing or lacking the *bk2-Mu1* mutant allele, respectively.

Cloning of *Bk2*

As we were identifying the tagged *bk2* gene by standard cosegregation analyses (Multani et al., 2003), a rice

bc1 mutant, whose brittle plant phenotype matches closely with that of the maize *bk2*, was reported (Li et al., 2003). Because *bc1* mapped to a region of the rice genome that exhibited a syntenic relationship with the maize region harboring *bk2*, we hypothesized that they may be related. Database searches for maize sequences with homology to the rice *Bc1* gene revealed a full-length EST that exhibited 87% identity with the rice *Bc1* cDNA (data not shown). A complete genomic clone corresponding to this EST was also found in The Institute for Genomic Research database and was named Zm*Bc1*.

Primers were designed from the Zm*Bc1* sequence and used to clone a part of the gene by PCR. A radiolabeled probe derived from this amplicon was hybridized to the same blots used earlier to map *bk2* using RFLP markers (Fig. 3A). No recombinants were found between Zm*Bc1* and the *bk2* brittle phenotype, suggesting that the two were closely linked. To address whether the *bk2* phenotype results from a mutation in Zm*Bc1*, we took advantage of the *bk2-Mu1* mutant allele. DNA isolated from this mutant was subjected to a reverse-genetics PCR-amplification test to assess if it was caused by insertion of a *Mu* element. Using the genomic Zm*Bc1* sequence as a guide, several primers were designed from the gene (Fig. 3B). We especially targeted the 5′ end of the gene for primers because *Mu* elements are known to insert preferentially in this gene region (May et al., 2003). Each of the Zm*Bc1*-specific primers were used in combination with a primer from the *Mu* terminal inverted repeat (TIR) to run PCR reactions in which the template DNA was derived from *bk2-Mu1*. PCR reactions yielding amplification products revealed that a *Mu* element was inserted 119 nucleotides upstream of the start codon of Zm*Bc1* in the *bk2-Mu1* mutant allele (Fig. 3B). Typical of *Mu* elements (May et al., 2003), a 9-bp duplication of the target site was found to flank this *Mu* insertion.

To show that the maize *bk2* and the rice *bc1* are orthologs, we demonstrated that the original mutant allele (*br2-ref*) also has a structural aberration that would disrupt the function of Zm*Bc1*. Primers were designed across the Zm*Bc1* gene sequence and used in different combinations to amplify various parts of the gene by PCR. These reactions resulted in the identification of a region within the Zm*Bc1* gene of the *bk2-ref* mutant allele that failed to amplify repeatedly under normal PCR conditions. To address the possibility of an insertion in this region, a long-range PCR reaction was used that led to an amplification of a product that was about 1 kb larger than the product from B73 genomic DNA. Sequencing of this PCR product revealed the presence of a 1,085 bp novel insertion within the second exon of Zm*Bc1* in the *bk2-ref* allele (Fig. 3C), thereby confirming a structural and functional relationship between the maize *Bk2* and the rice *Bc1* genes.

The coding region of the *Bk2* gene (Zm*Bc1*) is 1,353 bp long and its predicted product has 84% and 70% identity with the rice BC1 and Arabidopsis COBL4 proteins, respectively (Fig. 4). In addition, the maize *Bk2* and rice *Bc1* genes comprise three exons with identical exon/intron boundaries. The predicted BK2 protein is 450 amino acids long in contrast to the 468 amino acids of BC1. BK2 and BC1 differ from each other substantially in the N-terminal signal peptide and the hydrophobic C-terminal sequence, the latter of which is predicted to be clipped at the ω-site following attachment of the GPI anchor in the endoplasmic reticulum (Li et al., 2003). The 26 amino acids, corresponding to locations 243 to 268 of BC1, are missing in BK2. A gap of 32 amino acids is at the same location in Arabidopsis COBL4 in relation to rice BC1.

Insertion in the *bk2-ref* Allele Uncovers a New and Unusual Family of Transposons

The insertion in *bk2-ref* reveals a new family of transposons with at least two unusual characteristics.

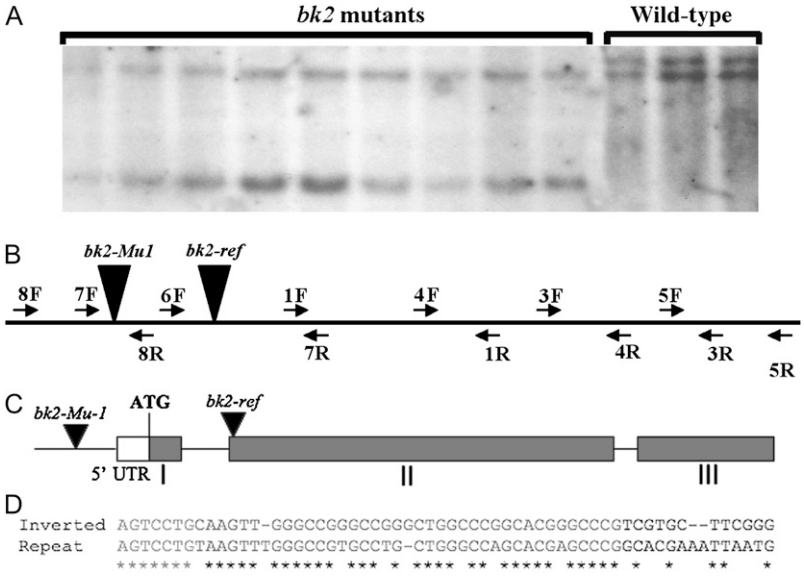

Figure 3. Cloning and confirmation of the *bk2* gene. A, Southern gel blot showing linkage of *bk2* with the maize homolog of the rice *Bc1* gene (Zm*Bc1*). B, The relative location of the two insertions (triangles) and of various primers (arrows) that were designed to amplify the *bk2* gene. C, Diagrammatic representation of the *bk2* gene showing three exons (gray rectangles), the relative location of the start codon (ATG), and the location of insertions (triangles) in the *bk2-Mu1* and *bk2-ref* mutant alleles. *Mu-1* is inserted 119 bp upstream of ATG, and the 5′ UTR is 90 bp long. D, The TIR of the novel insertion in the *bk2-ref* allele. Out of 46 bases, only the terminal 7 bp exhibit perfect identity.

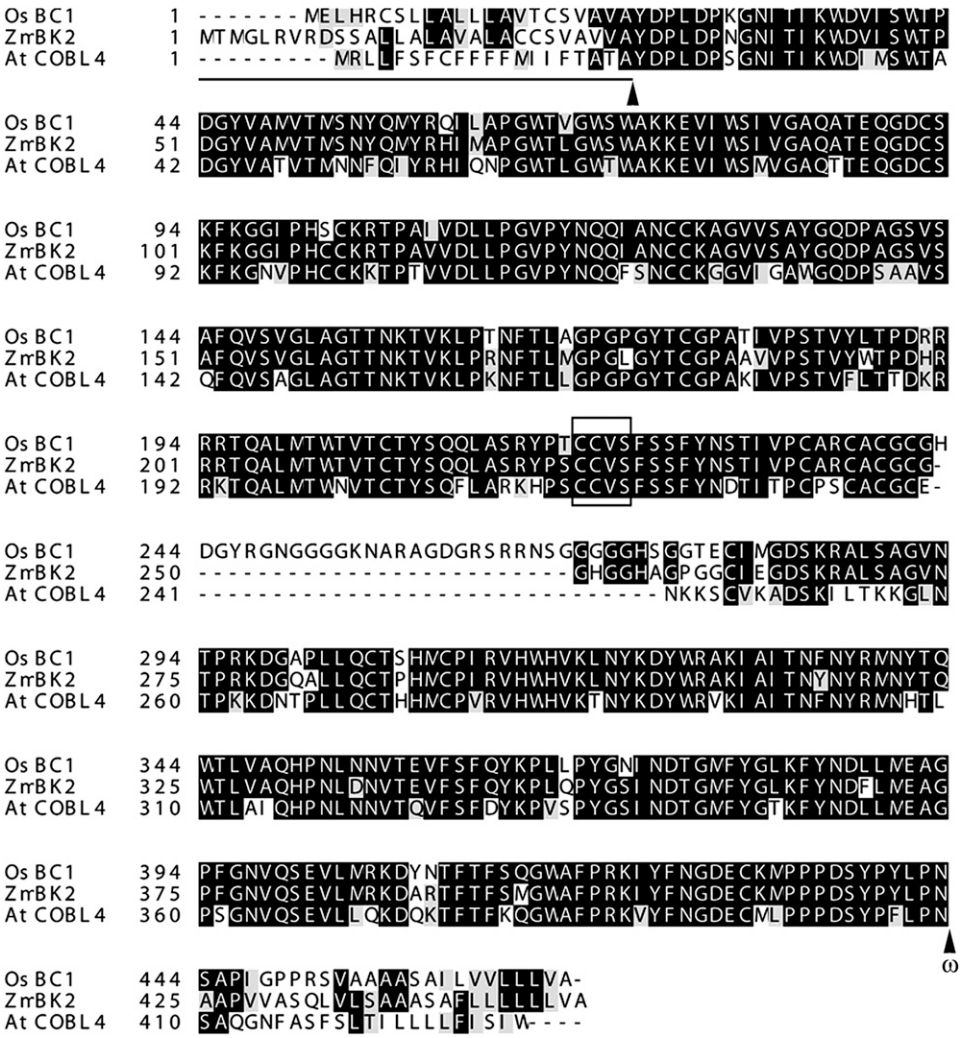

Figure 4. Protein sequence alignment of ZmBK2, OsBC1, and AtCOBL4. Numbers at the left are the positions of the amino acids in each protein, with gaps (dashes) included to maximize alignments. Identical and similar amino acids are shaded in black and gray, respectively. The predicted signal peptide is underlined, with cleavage site marked by an arrowhead. A consensus amino-acid sequence CCVS in all COBL proteins is boxed. The ω-amino acid at the predicted GPI cleavage site is denoted by an arrowhead.

First, they have an imperfect TIR of 46 bp, of which only the outermost 7 bp exhibit a perfect match between the left and the right borders (Fig. 3D). Second, they cause a 10-bp duplication at the site of insertion, another novelty among the transposable elements identified thus far in plants. However, Ching et al. (2006), who also cloned this insertion and named it KITE, reported this duplication to be of 8 bp. About 50 copies of KITE have been detected in the maize databases. Southern blots have also revealed equivalent copies of this tranposon in most maize inbreds and in Teosinte (data not shown). Hundreds of copies of a modified version of KITE have also been detected in the rice genome (A. Sindhu and G. Johal, unpublished data).

The *bk2* Brittle Phenotype Is Independent of Tensile Strength

Sections of wild-type and *bk2* leaves were tested for break strength. Thin sections of leaves taken parallel to the vascular tissue broke at a force about twice that of leaf sections made perpendicularly, but the average breaking strengths of wild type and *bk2* were indistinguishable (Fig. 5A). Similarly, the strain profiles in a one-point bend test of internodes of wild type and *bk2* were indistinguishable. Whereas the wild type only bent upon increasing stress, the *bk2* internodes snapped at variable points beyond the maximum stress exerted (Fig. 5B). These results contrast with those of Ching et al. (2006), who reported a difference in the strain curves. We found that the strain was quite variable among samples from both wild type and *bk2*, but the average maximum force required to crease the tissue was about the same (Fig. 5, A and B, insets). Whereas *bk2* snapped, wild type continued to bend with continually less resistance to the displacement. Whether interpreted as a consequence of a loss of mechanical strength (Ching et al., 2006) or flexibility, these results indicate an architectural defect in the cell walls of the *bk2* mutant (Fig. 5B).

bk2 Exhibits Abnormalities in Cell Wall and Cellulose Deposition in Leaves and Mature Stem

We characterized cellulose and noncellulosic monosaccharide distributions in the leaf and internode

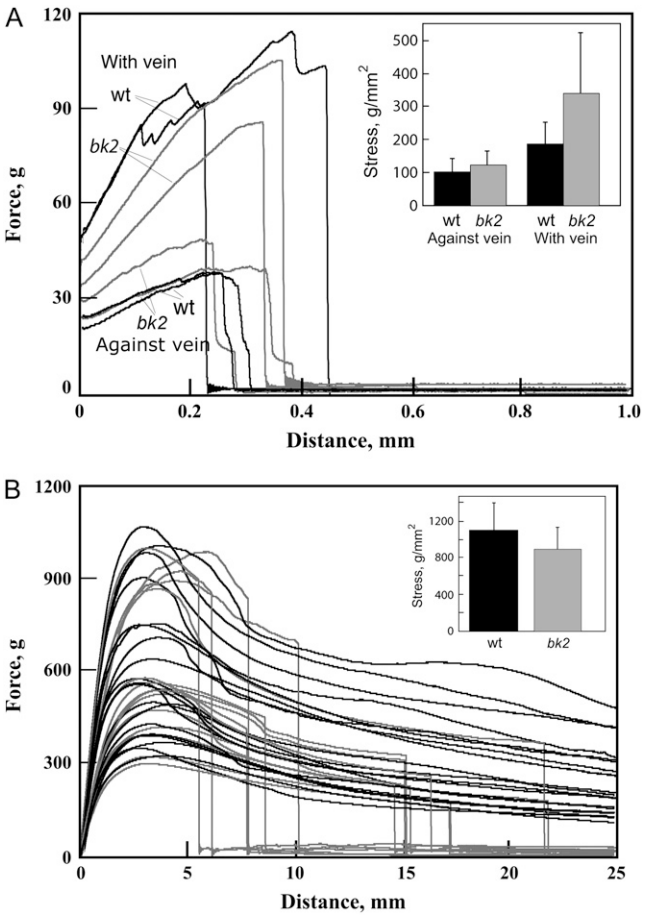

Figure 5. Mechanical strength and flexibility of leaves and internodes. A, Examples of stress-strain curves of force versus displacement for *bk2* and wild-type leaf sections taken parallel (with vein) and perpendicular (against vein) to the long axis of the leaf blade. Inset, Average values and SD ($n = 11–13$ samples) for maximum force before breakage for the *bk2* and wild-type leaves. B, Examples of stress-strain curves of force versus displacement for *bk2* and wild-type stems in a one-point bend test. While both *bk2* and wild-type stems reach a maximum force by about 4 mm, all *bk2* stems snap at some point upon continued bending, observed as the sudden loss of force applied. Inset, Average values and SDs ($n = 22$ for wild type, $n = 20$ for *bk2*), where *F* is determined as the maximum force tolerated before severe bending.

walls of *bk2* and wild-type plants at stages before and after the brittle phenotype developed. Leaf and internode tissues were pulverized in liquid nitrogen, portions were freeze-dried directly to give total dry mass of the tissue, and cell walls were isolated from the remaining material. Relative cellulose content could be quantified as a proportion of the total dry mass and total cell wall mass (Fig. 6, A and B). Before the appearance of the brittle phenotype, only the juvenile leaves are present and little difference in proportions of wall mass or cellulose content were observed (data not shown). After the appearance of the phenotype, wild-type cellulose mass represents 13% to 17% of the total dry mass of the juvenile and adult leaves and 13% to 19% of the dry mass of the stem, and in each tissue the reduction in cellulose is more drastic with increased maturity of the tissues (Fig. 6A). In contrast, the proportions of the cell wall mass per total dry mass were greater in *bk2* than in wild type (Fig. 6A). The proportion of cell wall cellulose varied from 31% to 39% in wild-type leaves and 23% to 33% in *bk2* leaves (Fig. 6B). However, while *bk2* exhibited a stark cellulose deficiency in the mature stem, the percentage cellulose in the cell walls of *bk2* developing stems was slightly greater than that of wild type.

Hydrolysis of isolated walls with 2 M trifluoroacetic acid (TFA) gives an insoluble residue, which is mostly cellulose, and soluble monosaccharides from noncellulosic polysaccharides. The monosaccharides, quantified

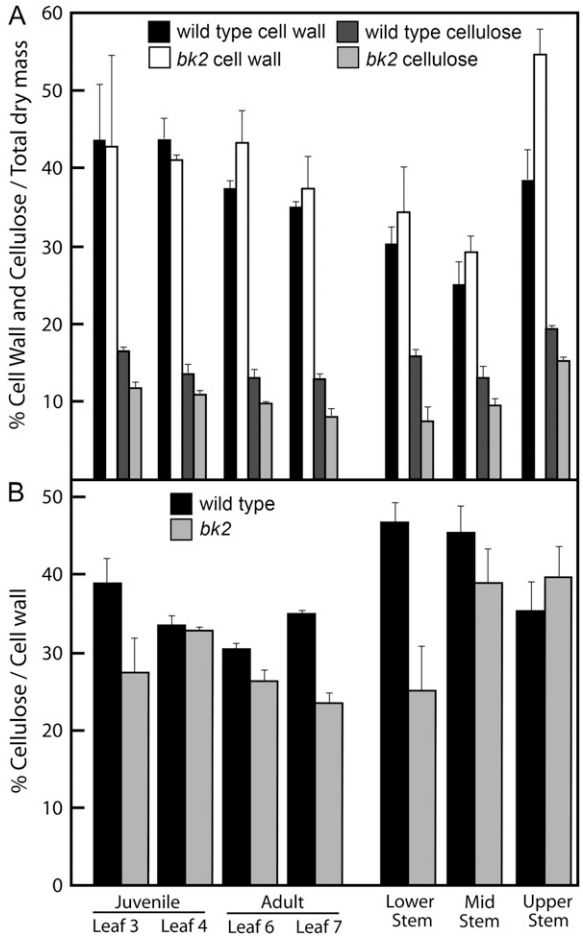

Figure 6. Determination of cell wall and cellulose content in juvenile leaves 3 and 4, adult leaves 6 and 7, and mature (S1, basal one-third) and developing internodes (S2, middle one-third, and S3, top one-third below the tassel stem) of wild type and *bk2* demonstrating the brittle phenotype. Samples of total mass and isolated walls were weighed and digested with acetic-nitric reagent (Updegraff, 1969). The undigested cellulose was pelleted by centrifugation and washed several times with water. Glc equivalents were determined by phenol-sulfuric acid assay (DuBois et al., 1956) and converted to weight amounts for determination of weight%. Error bars are the mean ± SD of at least four samples. A, Cell wall and cellulose content is calculated as weight% of the total dry mass. B, Cellulose content is calculated as dry mass of isolated cell walls.

by separation as alditol acetates, give an estimate of the relative abundance of the major wall constituents. With increasing maturity of leaves, Xyl content was higher in proportion relative to all other monosaccharides and with a slight increase in Xyl at the expense of Glc in *bk2* leaves relative to wild type after the brittle phenotype develops (Fig. 7, A and B). These results indicate that the increase in relative wall mass to dry mass (Fig. 6A) involves an increased synthesis of xylans.

Analysis of Secondary Wall Architecture by Fourier Transform Infrared Spectroscopy

Using scanning electron microscopy, we observed specific decreases in secondary wall thickness in sclerids of the rind and surrounding vascular bundles in the *bk2* stem (Fig. 2, G and H). We used Fourier transform infrared (FTIR) microspectroscopy to assess wall phenotypes in isolated cell walls from juvenile and adult leaves, and from sclerid-enriched fragments of the rind of mature and developing internodes. FTIR spectroscopy is a vibrational spectroscopic method that can quantitatively detect, without derivatization, the relative amounts of functional groups, including carboxylate esters, phenolic esters, amides and carboxylic acids, and a carbohydrate fingerprint region, with absorbances at certain wave number serving as diagnostic of cellulose, cross-linking glycans, and pectins in maize and other grasses (Tsuboi, 1957; Liang and Marchessault 1959; Séné et al., 1994; Carpita et al., 2001). Thirty to 40 spectra were obtained from wild-type and *bk2* plants for each organ and developmental stage. The spectra of cell walls from internodes and leaves were similar, but there were differences between walls of *bk2* and wild type for these tissues (Fig. 8). Consistent with chemical analyses of cellulose (Fig. 6B), the digital subtraction spectra, subtracting the average spectrum of *bk2* walls from that of wild type, show wild-type mature stems are relatively enriched in absorbances characteristic of cellulose (wave numbers 1,157, 1,108, and 1,061 cm^{-1}) and that of phenolic esters (wave number 1,728 cm^{-1}) is relatively enriched in *bk2* (Fig. 8B). A cellulose deficiency is also observed in *bk2* adult leaves, but comparison of digital subtraction spectra of the immature stems and juvenile leaves do not indicate a substantial deficiency in the *bk2* mutant (Fig. 8, D, F, and H).

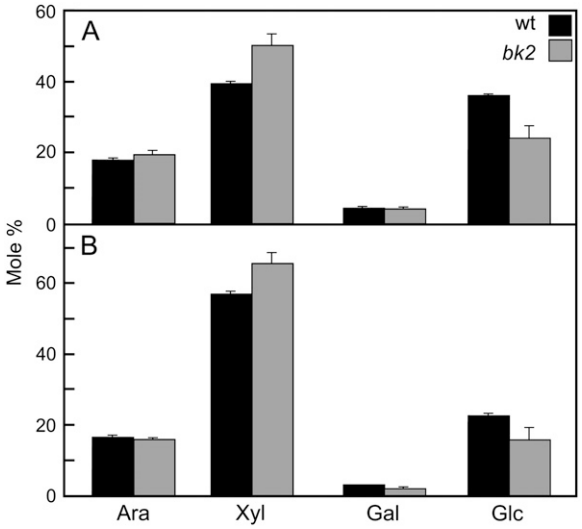

Figure 7. Noncellulosic cell wall monosaccharide distributions of wild-type and *bk2* juvenile and adult leaves after appearance of the brittle phenotype. Samples are digested with 2 M TFA at 120°C for 90 min to hydrolyzed noncellulosic polysaccharides to monosaccharides. The TFA is evaporated, and alditol acetates derivatives are separated and quantified by gas-liquid chromatography. Mol% was calculated based on response-factor values of standards treated similarly during derivatization. A, Juvenile leaves (leaf 3). B, Adult leaves (leaf 6).

Principal components analysis applied to populations of spectra taken from isolated walls of wild-type and *bk2* mature basal internodes showed that over 90% discrimination could be obtained using only three PCs (Fig. 9, A and B). The wild-type population was enriched in PC1, the loading for which has absorbances of 1,034, 1,057, 1,108, and 1,157 cm^{-1}, characteristic of cellulose. In contrast, the walls of *bk2* mature internodes had higher PC3 scores, the loading for which has absorbances at 1,728 to 1,732 cm^{-1} and 1,234 to 1,242 cm^{-1}, which are characteristic of phenolic esters. A similar PC1 loading was obtained when spectra from cell walls of *bk2* juvenile and immature internodes of were compared to those of wild type, but PC1 scores did not contribute to discrimination of the two populations (under 60% correct assignment using PC1 for either group). However, spectra derived from walls of *bk2* immature stems and juvenile leaves were significantly discriminated from wild type by PC3, for which loading 3 demonstrates an enrichment in phenolic esters in *bk2* (Fig. 9, D and F). Whereas discrimination of *bk2* and wild-type cell walls of the internodes and juvenile leaves was nearly 80% using three PCs, the spectra from cell walls of adult leaves were poorly discriminated. However, marked increases in discrimination of the walls of adult leaves were achieved using up to five PCs, with PC loading 5 having absorbances at 1,728 and 1,238 cm^{-1} associated with an enrichment of phenolic esters in the *bk2* (Fig. 9H).

Qualitative and Quantitative Changes in Lignin and Hydroxycinnamic Acids

Whereas the relative proportion of Klason lignin in juvenile leaves is essentially unchanged before or after the appearance of the brittle phenotype, lignin was markedly enriched in the cell walls of *bk2* mature and developing stems (Fig. 10). Despite this enrichment in total content, there is significantly less phloroglucinol-staining material in the mutant stem slices and sections compared to those derived from wild-type siblings (Fig. 11, A–C). This staining difference is only detected in the mature stems, as developing stems of both *bk2* and wild-type tissues do not stain. Consistent with these

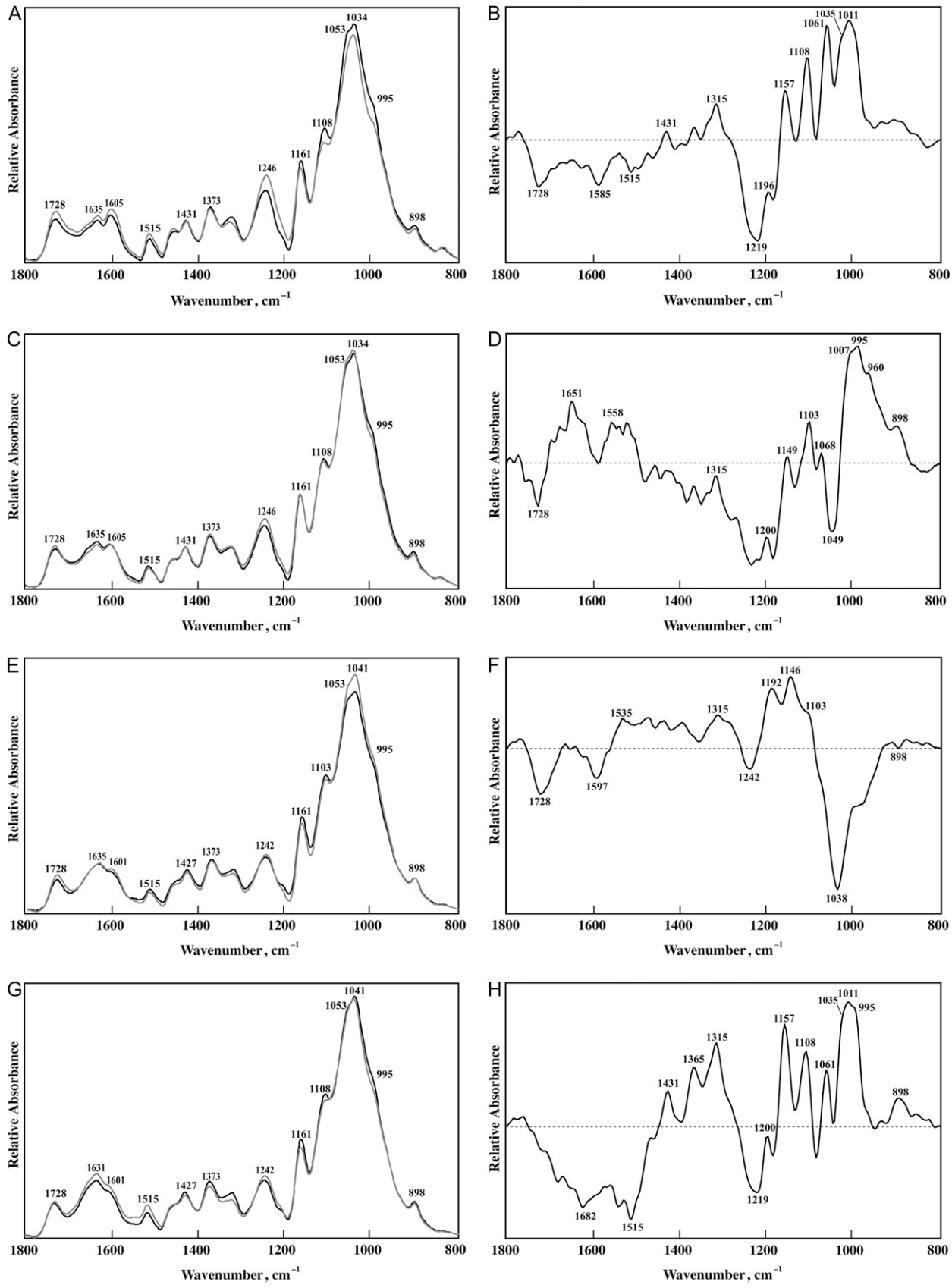

Figure 8. (*Legend appears on following page.*)

results, we found that cell walls of mature *bk2* stems were less autofluorescent than wild type when viewed under UV light (Fig. 11, D and E). These results are consistent with enhanced levels of Klason lignin observed in rice *bc1* but differ in the Wiesner (phloroglucinol)-staining behavior (Li et al., 2003). The total amounts of extractable UV-absorbing esterified hydroxycinnamates, primarily *p*-coumarate, ferulate, and other phenolic substances released upon saponification of isolated walls, were significantly higher in *bk2* than in wild type in all tissues (Table I). Whereas comparable amounts of *p*-coumaric and ferulic acid (FA) were found in leaves, the stems had substantially higher amounts of *p*-coumaric acid (*p*CA) than FA. These results are consistent with the finding of higher levels of phenolic esters by infrared spectroscopy (Figs. 8 and 9).

Comparison of normalized mass spectral data obtained after pyrolysis of isolated cell wall material from the developing internode indicated that the chemical composition of mutant and wild type were similar (Table II). Based on the increase in the intensity of mass-to-charge ratio (*m*/*z*) 73, 85, and 114, *bk2* contains slightly more pentose-based polysaccharides (arabinoxylans) but the content of cellulose is unchanged (*m*/*z* 126, 144). The mutant contains less total *p*CA (*m*/*z* 164, 147) but a higher amount of FA (*m*/*z* 194). In contrast, the cell walls of mature stems of the *bk2* mutant contain more lignin and more *p*CA and FA, confirming the results from the lignin content analysis and the HPLC analyses of saponified cell walls. The peak intensity corresponding to lignin-derived compounds was 30% to 40% higher in *bk2*, whereas the peak intensities of polysaccharide indicators did not change or were only slightly higher. The peak intensities of compounds derived from both guaiacyl (G; *m*/*z* 137, 151, 152, 178, 180) and syringyl (S; *m*/*z* 153, 165, 167, 208, 210) residues were increased in the *bk2* mutant, but the ratios of S to G, calculated for two pairs of selected compounds representing each subunit, were nearly constant. Since *p*CA is primarily esterified to S residues (Ralph et al., 1994), the increase in *p*CA in the stems of *bk2* after the brittle phenotype manifests itself can therefore be largely attributed to the increase in lignin content. Analysis of the cell wall composition of the juvenile leaf of wild-type and *bk2* plants shows similar small differences in composition between wild type and *bk2* as was observed in the internode tissue from the developing stems.

Bk2 Is Expressed Strongly Only during Early Development

Reverse transcriptase-coupled PCR (RT-PCR) was used to examine the transcriptional pattern of *Bk2* using gene-specific primers. *Bk2* was expressed in most parts of the maize plant (B73 inbred) including roots, shoots, and stems. However, no RT-PCR product could be amplified from plants homozygous either for *bk2-ref* or *bk2-Mu1*, indicating that both of these mutant alleles are null.

To address how the expression of the *Bk2* gene relates to the developmentally specified phenotype of the mutant, total RNA was also extracted from leaves of B73 at weeks 1, 2, 3, 4, and 8 and subjected to semiquantitative RT-PCR. *Bk2* transcripts are more abundant at early stages of growth (weeks 1 and 2) than at later stages (weeks 3, 4, and 8; Fig. 12). Northern gelblot analyses of poly$A^{(+)}$-RNA confirmed a higher transcript level at weeks 1 and 2 with transcript abundance markedly decreasing in weeks 3 and 4 (Fig. 12).

DISCUSSION

Bk2 Encodes a COBL Protein

Mutations in the *COB* gene of Arabidopsis were so named because of a change in the orientation of cell expansion in the root from the longitudinal axis to the radial axis, widening the root diameter progressively away from the tip and giving roots the appearance of a the head of a cobra (Hauser et al., 1995). Because this change in orientation was accompanied by a drastic lowering in the crystalline cellulose in the root cell walls, Schindelman et al. (2001) suggested that COB is either directly or indirectly involved in cellulose synthesis. The *COB* gene was identified by map-based cloning and predicted to contain an N-terminal signal sequence for secretion, a highly hydrophobic C-terminal sequence, and a GPI anchor sequence near the C terminus (Udenfriend and Kodukula, 1995a).

The cleavage site in known GPI-anchored proteins, termed ω, contains only Ser, Asn, Ala, Gly, Asp, and Cys, with only Ala, Gly, Thr, and Ser found at the +2 site (Udenfriend and Kodukula, 1995b). The +2 residue of known GPI-anchored proteins is usually followed by a spacer of five to seven amino acids rich in charged and/or Pro residues followed, in this instance, by a stretch of 20 to 25 hydrophobic residues. The ZmBK2 meets these criteria, with Asn at the ω site and Ala occupying the +2 position, and a Pro at the +3 position (Fig. 4). The 12-member Arabidopsis *COBL* gene families are all predicted to encode GPI-anchored proteins. With the exception of two members, *COBL6* and *COBL9*, whose expression is floral specific, the rest of the *COBL* genes are expressed to different extents in

Figure 8. Averaged FTIR spectra (A, C, E, and G) and digital subtraction spectra (B, D, F, and H) of isolated cell walls of wild-type and *bk2* organs after the appearance of the brittle phenotype. In all spectra, wild-type spectra are in black, and *bk2* are in gray scale. A and B, Mature basal internodes at tasseling. C and D, Developing internode taken just below the tassel internode. E and F, Juvenile leaves (leaf 3). G and H, Adult leaves (leaf 7).

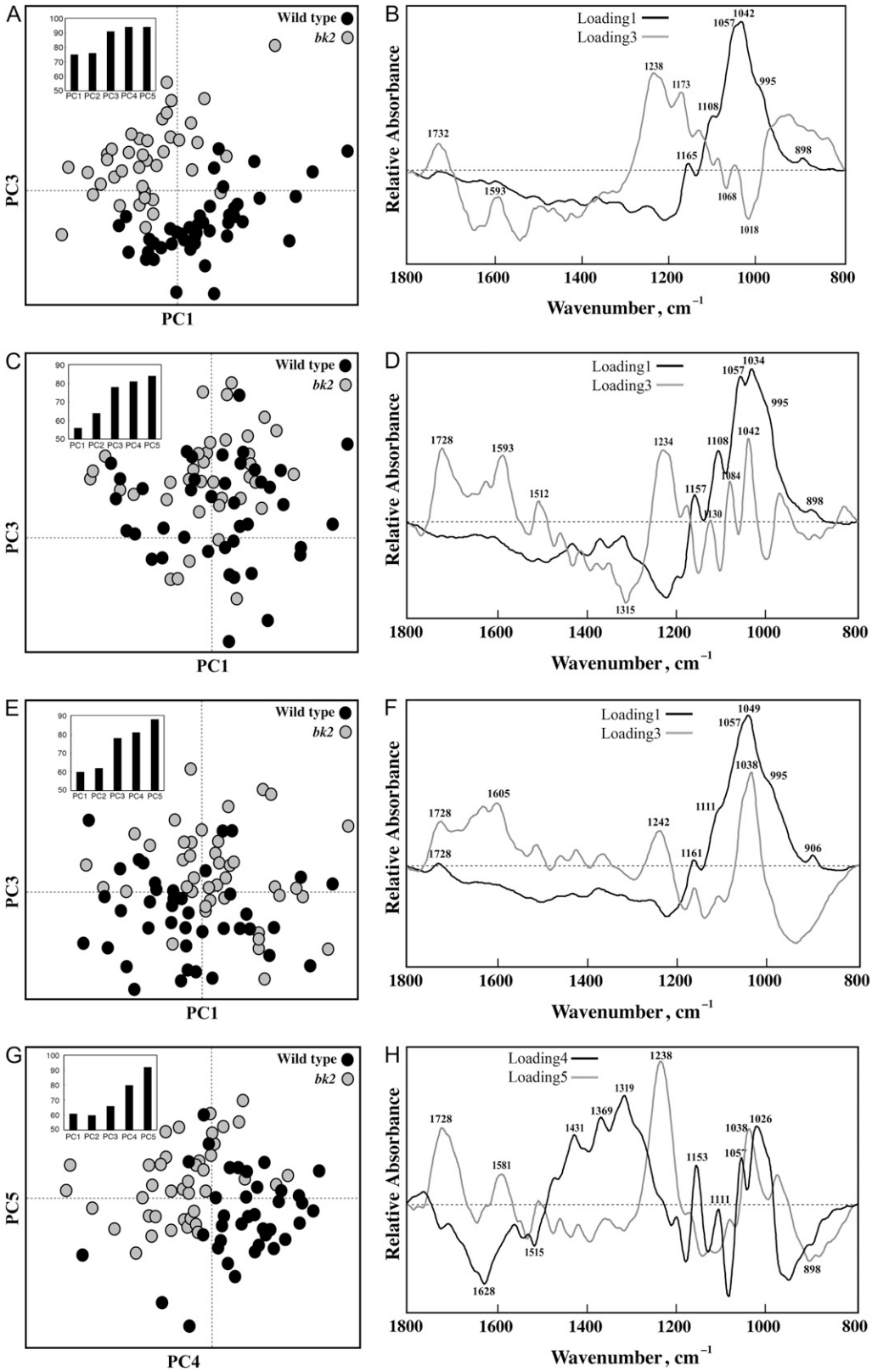

Figure 9. Principal components analysis of FTIR spectra of cell walls of wild-type and *bk2* leaves and stems after the appearance of the brittle phenotype. PC scores plots and PC loadings 1 and 3 of walls of *bk2* and wild type from: A and B, mature basal internode; C and D, developing internode just below the tassel internode; E and F, juvenile leaves (leaf 3). G and H, Loadings 4 and 5 of walls of *bk2* and wild-type adult leaves (leaf 7). Insets: Values reflect the classification percentages of populations of wild-type and *bk2* samples from the first five PC scores. A value of 50% means the populations cannot be discriminated.

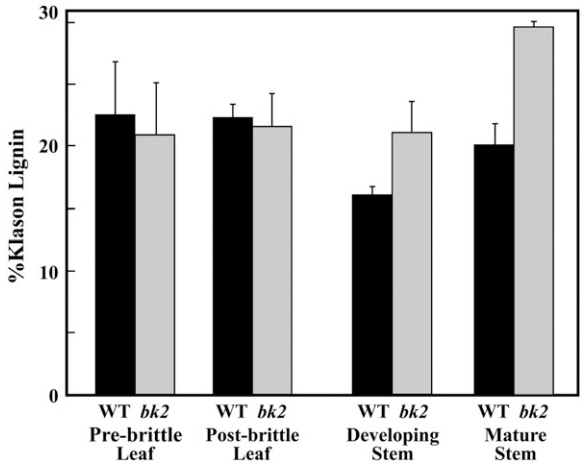

Figure 10. Klason lignin determination of cell walls of juvenile leaves before and after appearance of the brittle phenotype and of mature and developing stems. Klason lignin was determined gravimetrically after correction for ash, according to Theander and Westerlund (1986), as modified by Hatfield et al. (1994). Values are mean ± SD of four samples.

all organs (Roudier et al., 2002). BK2 is most closely related to the rice BC1 and Arabidopsis COBL4, with 88% and 70% identity, respectively. The rice BC1 has a unique 25-amino acid insertion rich in Gly residues that is absent from both maize BK2 and Arabidopsis COBL4 proteins (Fig. 4).

Similar to other COBL proteins, BK2 possesses a conserved region between amino acids 53 to 217, characteristic of a metal-binding domain of plant phytochelatin synthases ($E = 3.6\ e^{-99}$, with 83%–91% similarity and 72%–80% identity to four plant phytochelatins). Leuchter et al. (1998) complemented the *Schizosaccharomyces pombe* mutant defective in phytochelatin synthesis by expressing partial *COB* cDNA, and wheat (*Triticum aestivum*) COB1 possesses phytochelatin synthase-like activity that improved resistance to cadmium when expressed in *Escherichia coli* (Wang et al., 2006). A set of conserved Cys residues involved in metal ion binding was also observed (Roudier et al., 2002). While it is unlikely that the COBL proteins function as phytochelatin synthases, the metal-binding domains may be conserved for an alternative function (Wang et al., 2006).

Amino acids 37 to 76 of BK2 also show weak similarity (7%–13%) to a family II cellulose-binding module related to that of several bacterial type II cellulases (Simpson et al., 2000), but the Trp residues found in this region are conserved in BK2 and COBL1-5, and, with the presence of an adjacent conserved Gly, is predicted to confer binding specificity to cellulose over xylan (Linder and Teeri, 1997). COBRA is one of several plant proteins predicted to be GPI anchored that have been solubilized from plasma membranes by a phophatidylinositol-dependent phospholipase C (Roudier et al., 2005). Others include several arabinogalactan proteins (Youl et al., 1998), other cell expansion orientation factors SKU5 (Sedbrook et al., 2002), and SOS5 (Shi et al., 2003), and several disparate types of proteins, including hydrolases, proteases, and receptor-like kinases (Borner et al., 2003).

Although mutation of COBRA and other GPI-anchored proteins affect orientation of expansion, this phenotype is not observed in either *bc1* or *bk2* mutants. A reduction in secondary cell wall deposition indicates that the activities of these COBL proteins may be restricted to wall deposition in specialized cells after elongation. An independent expression-profiling study showed that the most closely related Arabidopsis COBL4 is coregulated with secondary wall cellulose synthases (Brown et al., 2005). Three independent insertional *cobl4* mutants exhibit an irregular xylem phenotype and display a brittle phenotype (Brown et al., 2005).

There are no reports of irregular xylem phenotypes in grass mutants. In dicots, defects in secondary cell wall formation, whether due to defects in cellulose

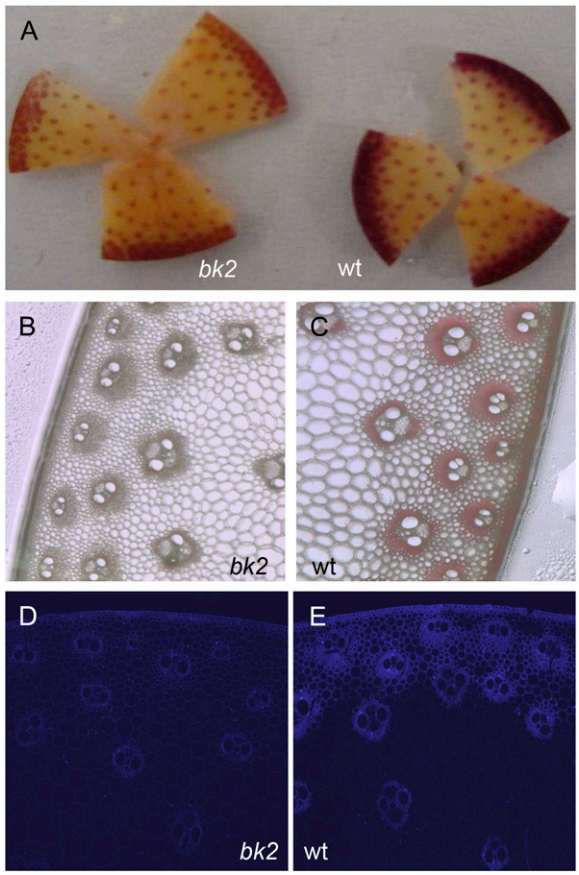

Figure 11. The quality of lignin is altered in *bk2*. A, Phloroglucinol staining of freshly-cut mutant (*bk2*) and wild-type (wt) stalk sections. B and C, A freshly-cut, phloroglucinol-stained transverse sections of *bk2* and wild-type stems. D and E, UV autofluorescence of sections from *bk2* and wild-type stems.

Table I. *Hydroxycinnamic acid content in the cell walls of bk2 and wild-type tissues*

*, Estimations of total hydroxycinnamates were based on contributions of ferulic and *p*CA as judged from their respective absorbance at 310 nm and the ratio of each assayed by HPLC.

Tissue	Total Hydroxycinnamates*	*p*-Coumarate	Ferulate	*p*-Coumarate/Ferulate
		nmol/mg cell wall		
Juvenile leaves				
Wild type	104 ± 4	38 ± 4	27 ± 2	1.38
bk2	126 ± 20	43 ± 3	40 ± 0	1.07
Adult leaves				
Wild type	118 ± 5	47 ± 1	38 ± 1	1.24
bk2	141 ± 13	66 ± 14	46 ± 3	1.43
Mature stem				
Wild type	244 ± 18	166 ± 3	37 ± 1	4.44
bk2	311 ± 2	204 ± 4	64 ± 15	3.17
Developing stem				
Wild type	202 ± 13	113 ± 7	37 ± 1	3.19
bk2	290 ± 18	140 ± 4	48 ± 4	2.92

synthases or other components, lead to the collapsed or irregular xylem phenotype (Turner et al., 2001). However, none of the cellulose-deficient *irx* cell wall mutants having defects in *CesA* genes has a brittle phenotype. Only *irx2*, defective in *KORRIGAN* (*KOR*), a membrane-associated endo-(1 → 4)-β-D-glucanase gene (Lane et al., 2001), and *cobl4*, defective in an ortholog of the rice *Bc1* and maize *Bk2* genes (Brown et al., 2005), exhibit brittleness in addition to the *irx* phenotype and reduced cellulose content. These results suggest that COBRA has a function distinct from a role in cellulose biogenesis.

Table II. *Pyrolysis-mass spectrometry of cell wall samples of developing and mature stems and juvenile leaves*

*, These ratios have not been corrected for the response factor and are therefore not reflective of the actual molar ratios. G, Guaiacyl units; S, syringyl units; pCA, *p*-Coumaryl units; FA, feruloyl units; wt, wild type.

m/z	Origin	Mature Stem		Develop. Stem		Leaves	
		wt	*bk2*	wt	*bk2*	wt	*bk2*
				Peak area %			
73	Polysaccharide	2.41	2.95	2.50	3.02	2.65	3.20
85	Polysaccharide	2.51	2.84	2.88	3.06	3.13	3.13
98	Polysaccharide	0.43	0.43	0.52	0.55	0.61	0.67
114	Pentose	1.06	1.29	1.69	1.62	1.47	1.47
126	Hexose	0.27	0.23	0.31	0.30	0.31	0.38
144	Hexose	0.13	0.11	0.20	0.21	0.87	0.75
137	Coniferyl alcohol $[M-43]^+$ (G)	1.51	1.50	0.73	0.97	0.22	0.26
147	pCA $[M-17]^+$	2.16	2.00	1.12	1.59	0.73	0.63
150	4-Vinylguaiacol (FA)	0.32	0.34	0.36	0.42	0.44	0.37
151	Vanillin (G)	0.84	0.83	0.52	0.71	0.53	0.55
152	Vanillin (G)	0.43	0.43	0.27	0.38	0.37	0.34
153	2,6-Dimethoxy-4-methylvinylphenol $[M-15]^+$ (S)	0.32	0.37	0.20	0.28	0.19	0.17
164	pCA; (iso)eugenol (G)	3.25	2.79	1.74	2.55	0.83	0.79
165	Sinapaldehyde $[M-43]^+$ (S); 2,6-dimethoxy-4-vinylphenol $[M-15]^+$ (S)	0.53	0.52	0.31	0.43	0.20	0.19
167	Sinapyl alcohol $[M-43]^+$ (S); syringyl acetone (S)	0.34	0.41	0.20	0.28	0.16	0.12
178	Coniferaldehyde (G)	0.57	0.57	0.36	0.42	0.36	0.36
180	Coniferyl alcohol (G); 2,6-dimethoxy-4-vinylphenol (S)	0.98	0.91	0.43	0.59	0.46	0.39
194	FA; 2,6 dimethoxy-propenylphenol (S)	0.33	0.49	0.34	0.44	0.29	0.37
208	Sinapaldehyde (S)	0.26	0.23	0.14	0.19	0.10	0.09
210	Sinapyl alcohol (S)	0.22	0.24	0.10	0.15	0.06	0.07
				*Ratios			
S/G	*m/z* 165/137	0.38	0.35	0.43	0.44	0.23	0.27
	m/z 153/151	0.38	0.46	0.38	0.40	0.35	0.30
pCA/S	*m/z* 164/165	6.13	5.42	5.50	5.89	5.01	6.70
	m/z 147/167	6.54	4.92	5.70	5.70	3.66	3.26

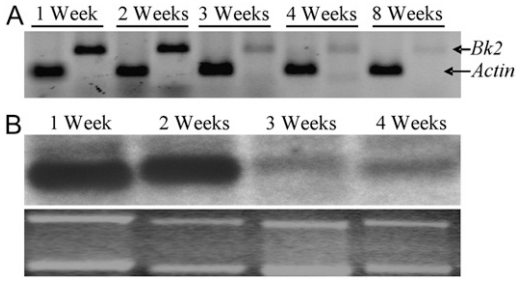

Figure 12. The *Bk2* gene is expressed much earlier than the appearance of the brittle phenotype. A, An RT-PCR assay showing that the expression of *Bk2* is higher during earlier stages of maize development. In contrast, the expression of the *Actin* gene in these samples remained unchanged. B, Northern-based expression analysis of *Bk2* confirming the RT-PCR data shown in A. PolyA$^{(+)}$-enriched RNA was used for the northern analysis. Gel blot in the lower section shows the relative amount of polyA$^{(+)}$ RNA in different samples. Leaf materials were pulverized in liquid nitrogen and RNA extracted from aliquots of the frozen powder. For RT-PCR analyses, the topmost fully expanded leaf was used; for polyA$^{(+)}$-enriched northern gel blots, the entire seedling or plants were used.

What Is Directly Responsible for the Brittle Phenotype?

The appearance of the brittle phenotype coincides with the transition from juvenile to adult leaves and a qualitative change in the deposition of lignin. This is apparent from various phase-change and *brown midrib* mutants (Moose and Sisco, 1994; Marita et al., 2003; Lauter et al., 2005). Whereas cellulose content is compromised in the *bk2* mutant (Fig. 6), lignin deposition is enhanced (Fig. 10). Lack of a proper cellulosic matrix in the secondary wall may lead to an aberrant lignin polymerization, rendering it incapable of withstanding bending stress.

Despite the drastic increase in lignin content of the *bk2* stems, acid phloroglucinol-stained material is reduced in the cells of these stems. This finding is in sharp contrast to that observed in rice (Li et al., 2003). These differences may be attributed to different lignin structures in different species with different stem architectures. Alternatively, the increases in lignin content may not be restricted to the vascular bundles and rind tissues in maize. Although the Wiesner stain reacts with cinnamaldehyde residues in lignin and the color intensity approximately reflects the total lignin content, our anomolous results indicate that there may be other changes in cell wall phenolics that contribute to cell wall flexibility. Our infrared analyses indicate that phenolic esters are increased in *bk2* relative to wild type. We measured increased levels of hydroxycinnamic acids in *bk2*, consistent with the increased amounts of (arabino) xylans. Ferulate esters attached to the arabinosyl units of the xylan become cross-linked into the lignin structure by diverse kinds of linkages (Iiyama et al., 1994). Coniferaldehyde is the precursor of FA (Nair et al., 2004) and enhanced ferulate ester production may drain the aldehyde pools, resulting in decreased phloroglucinol staining.

Bk2 Expression Prestages the Appearance of Phenotype

Consistent with a secondary wall function, rice *Bc1* demonstrates expression associated primarily with vascular bundles and the rind (Li et al., 2003). However, maize *Bk2* expression is highest very early in leaf development but greatly reduced when the brittle phenotype presents itself (Fig. 12). The decrease in cellulose but not wall mass occurs in leaves before the onset of the brittle phenotype, and while it may predispose the organs to the brittle nature, it cannot be the direct cause. Such an expression pattern was observed not only when whole seedlings/plants were examined, but also when different plant parts such as leaf blades, leaf sheaths, or tiny stems were excised and examined separately (data not shown). Given the anatomical alterations in vascular bundle distribution as well as secondary wall defects, early expression predisposes the tissues to brittleness long before the onset of the actual phenotype. In line with our findings, *Bc1* also expresses most strongly in tiller buds, long before they develop sclerenchyma cells (Li et al., 2003).

Does BK2 function similarly to other COBL proteins that function during primary wall growth and cellulose deposition? Alterations in cell walls can be an indirect consequence of mutations in more global developmental programs and expression of cell wall-related genes is modified in many different signal transduction pathways. Therefore, a cell wall mutant phenotype is not necessarily a result of a mutation in a gene directly involved in cell wall synthesis or assembly. For example, cellulose deficiency is a consequence of several kinds of mutations other than a defect in cellulose synthase catalytic subunits. Mutations in another plasma membrane-associated protein, *kobito* (Pagant et al., 2002), an endoglucanase, *kor* (Nicol et al., 1998), and a katanin-like microtubule-severing protein *fra2* (Burk and Ye, 2002), all result in cellulose deficiencies. Further, plants also compensate cellulose deficiencies by altered wall metabolism. For example, tomato and tobacco (*Nicotiana tabacum*) cells with type I walls habituated to grow in cellulose synthesis inhibitors increased pectin cross-linking, whereas barley cells with type II walls do so by increased phenolic cross-linking (Shedletzky et al., 1992). Thus, one should not infer that all of these genes have a primary function in the biosynthesis of cellulose but that several pathways may regulate cellulose biosynthesis as a downstream target. The observation that total wall mass actually increases as cellulose is lowered in *bk2* (Fig. 6A) indicates that COBLs function in global integration of wall extension and deposition rather than directly in cellulose synthesis. The location of COBRA proteins at the interface of plasma membrane and cell wall and their association with lipid microdomains (rafts) suggest a potential integrative function in regulation or integration of secretion and wall assembly (Martin et al., 2005).

MATERIALS AND METHODS

Plant Material

The maize (*Zea mays*) mutant *bk2* was obtained from the Maize Genetics Cooperative as a stock (no. 916C) that had been maintained over many generations as a backcross progeny. To have a uniform background, the material was propagated by backcrossing *bk2* mutants with their wild-type heterozygotes an additional five times. These backcrosses resulted in a uniform background where the mutant (*bk2*/*bk2* homozygotes) and wild-type plants (*bk2*/+ heterozygotes) were indistinguishable from each other except for the appearance of a brittle phenotype at 4 weeks in the *bk2* mutants. In this backcross progeny, the mutant and wild-type plants segregated in a 1:1 ratio of homozygotes to heterozygotes. Upon harvest of plant material, it was frozen immediately with liquid nitrogen before being placed at −80°C until all samples had been collected.

Identification of RFLP Markers Flanking *bk2*

We generated another backcross population of *bk2* with B73. One hundred and fifty plants from this population were assessed for the brittle phenotype, as well as the genotype of a number of RFLP markers known to map in the vicinity of *bk2* on the proximal part of the long arm of chromosome 9. The data obtained placed *bk2* between *UMC95* and *BNL8.17*, with *BNL8.17* being 4.0 cM proximal and *UMC95* 2.5 cM distal to the *bk2* locus.

Southern and Northern Gel-Blot Analyses and PCR

DNA extraction and Southern gel-blot analyses were done as described before (Multani et al., 2003). For RNA, leaf materials were collected in bags and immediately frozen in liquid nitrogen and stored at −80°C. For RT-PCR analyses, the topmost fully expanded leaves at each age were used, whereas for polyA-enriched northern gel blots, the entire seedling or plants were used. Before extraction, the leaf materials were pulverized in liquid nitrogen and RNA extracted from aliquots of the frozen powder. Total RNA was extracted using $LiCl_2$ precipitation, as described by Lagrimini et al. (1987). $PolyA^{(+)}$ mRNA fraction was isolated from total RNA using the PolyATract mRNA Isolation System II kit from Promega. For northern gel-blot analysis, the $PolyA^{(+)}$ enriched RNA was fractionated on 1.2% (w/v) agarose gels. Samples of uniform quantity were prepared and mixed with 2× loading dye (547 μL of formamide, 182.5 μL of formaldehyde, 200 μL of 10× MOPS buffer {200 mM MOPS[Na], pH 7.0, containing 80 mM sodium acetate}, 66 μL of glycerol, 4 μL of 0.5 M EDTA, 5 μL of 10 mg mL^{-1} EtBr), and heated for 65°C to 70°C for 10 min and then immediately placed in ice before loading. Transfer, hybridization, and subsequent exposure of blots to x-ray films were as described in Multani et al. (2003).

The PCR reaction conditions and the *Mu*-TIR primer to seek the insertion of a *Mu* element in *bk2-Mu1* were essentially as described before (Multani et al., 2003), except we added 5% glycerol to the reaction mixture. Various *bk2*-specific primers used in this study were: 1F, 5′-GCGATGGTGACGATGAGCAAC-3′; 3F, 5′-ACTGGCACGTCAAGCTCAAC-3′; 4F, 5′-TGCGTCTCCTTCTCCTCCTTC-3′; http://www.idtdna.com/analyzer/Applications/Instructions/Default.aspx?AnalyzerDefinitions=true - MeltTemp; 5F, 5′-GGACTCCTACCCCTACCTGC-3′; 6F, 5′-TGCACACACACTGGCACTTG-3′; http://www.idtdna.com/analyzer/Applications/Instructions/Default.aspx?AnalyzerDefinitions=true - MeltTemp; 7F, 5′-TTTTATTCGCCCTGCCTCTAG-3′; 8F, 5′-ATCTAGCTGTGCCTGTGCCTG-3′; 1R, 5′-CGATGGTGCTGTTGTAGAAGGAG-3′; http://www.idtdna.com/analyzer/Applications/Instructions/Default.aspx?AnalyzerDefinitions=true - MeltTemp; 3R, 5′-ACCAGGAGCAGCAACAGTAGG-3′; 4R, 5′-TTGAGCCCGTAGAACATGCC-3′; 5R, 5′-GGGTTAGCAAATGTTCAGGCAAC-3′; 7R, 5′-ATGGACCAGATCACCTCCTTC-3′; 8R, 5′-ATGGTAACCGAACCTGCAACG-3′.

To elucidate the molecular nature of the structural polymorphism in *bk2-ref*, the Expand High Fidelity PCR system of Roche was used. The reaction conditions were set up as recommended by the manufacturer, except for the addition of 5% (v/v) glycerol. The cycle was repeated 30 times and the final elongation time was 15 min at 72°C. All amplified fragments were cloned in the pGEM-T vector from Promega.

For RT-PCR, total RNA was isolated from greenhouse-grown B73 plants and 1 μg of total RNA was used for each reaction for all samples. The first strand of cDNA was synthesized using the RETROscript kit from Ambion, essentially as described by the manufacturer. Next, 5 μL from each primary reaction was used for the second-step PCR reaction using *bk2*-specific primers 1F and 1R. RT-PCR controls were derived from the actin gene that was amplified using the following primers: forward primer 5′-TGTTTCGCCTGAAGATCACCCTGTG-3′; reverse primer 5′-TGAACCTTTCTGACCCAATGGTGATGA-3′.

Light and Scanning Electron Microscopies

The third stalk internode of greenhouse-grown plants at anthesis was used for microscopy. For scanning electron microscopy, stalk slices (approximately 1 mm in height) were prepared with a sharp razor and observed directly with a JFM-840 SEM (JEOL). For light microscopy, stalk slices were cut with a razor blade and fixed in 3% glutaraldehyde in 0.1 M potassium phosphate buffer, pH 6.8, under low vacuum in the desiccators overnight. Following dehydration, the samples were embedded in JB-4 resin following manufacturer's instructions (Electron Microscopy Sciences), and then sectioned (5-μm thickness) using a SORVALL type JB-4 Porter-Blum microtome (DuPont Company). The sections were dropped into a water bath (approximately 60°C) to expand them and four slides containing three to four sections each were prepared for each sample. They were either viewed under bright field or UV for autofluorescence (Nikon E800 Fluorescence Microscope; Fryer Company). For lignin staining, stalk slices were cut freehand and then stained with Wiesner's solution (2%, w/v) phloroglucinol in ethanol:50% HCl (v/v) in water (95:5, v/v). Samples of material were stained immediately or were first fixed in formalin-acetic acid-ethanol overnight before staining, and imaged with either Olympus Vanox-S brightfield or Nikon SMZ-U stereo microscope.

Leaf and Internode Tensile Strength Measurements

The tensile strength of *bk2* and wild-type leaves was tested using a tensile grip probe with a TA.XT*plus* texture analyzer (Texture Technologies) on 2-month-old sections from the sixth leaf (counted from the bottom). Leaf sections (2 mm × 20 mm), avoiding the midrib and major veins, were cut with razor blades either parallel or perpendicular to the minor veins. The thickness of the leaf was measured with a Nikon SMZ 1500 microscope. The leaf section ends were firmly attached to tensile grip plates with an inelastic adhesive (Advanced Formula Instant Krazy glue), leaving a 5-mm gap between the plates. The tensile grip plates were moved apart at 0.1 mm per second. The Texture Exponent 32 version 4 software displayed fracture breakage of the leaf as distance (mm) by force (g). Maximum stress tolerated before breakage was calculated from force measured at breakage and the total tissue load-bearing volume.

A simple one-point bend test was performed to determine brittleness of *bk2* and wild-type internodes. Individual fresh stem sections 20-cm long were cut, and the diameters of the cut section ends were measured with a Nikon SMZ 1500 microscope. The one-point bend rig was attached to the TA.XT*plus* texture analyzer and the probe was raised to a defined height and calibrated. The stem section was placed across two supports of the rig 40 mm apart, with 20 mm on either side of the supports. The probe for the one-point bend test moved toward the sample at a speed of 0.5 mm per second. Stress at fracture was calculated according to the equation:

$$\sigma = \frac{8FL}{\pi d^3}$$

where σ is the stress at fracture, F is the maximum force before deformation, L is the distance between the supports, and d is the stem diameter (Timoshenko and Young, 1962).

Cell Wall Isolation

The cell walls of various maize tissue samples were pulverized in liquid nitrogen with a mortar and pestle and divided into two portions. One was freeze dried to yield total dry mass, and for the second, cell walls were isolated by homogenization in 1% SDS in 50 mM Tris[HCl], pH 7.2, with a glass-glass motorized grinder (Kontes-Duall, Thomas Scientific). The samples were then heated at 80°C in 1% SDS for 15 min. All samples were washed five times with water through centrifugation and pelleting before the cells were broken again with the glass-glass motorized grinder. Samples were washed three times with water, two times with warm 50% ethanol, and three times with water. The remaining pellet was resuspended in water and freeze dried.

Determination of Cellulose, Lignin, and Saponifiable Phenolic Substances

Samples of total dry mass, ethanol-extracted material, and isolated cell walls were assayed for cellulose by acetic-nitric assay (Updegraff, 1969). Briefly, a known weight of isolated cell walls was hydrolyzed in 3 mL of acetic acid-nitric acid in water (8:2:1, v/v/v) at 100°C for 90 min in sealed 5-mL conical Reacti-vials (Pierce Chemical). The insoluble materials (mostly cellulose) were then pelleted by centrifugation and the pellet was washed five times with water. Cellulose in the pellet was assayed for Glc equivalents by phenol-sulfuric colorimetric assay (Dubois et al., 1956). Klason lignin determinations were performed as described by Theander and Westerlund (1986) as modified (Hatfield et al., 1994). To determine total saponifiable hydroxycinnamates and other phenolic substances, isolated walls were suspended in 1 M NaOH for 30 min at 37°C. After cooling, HCl was added to 1 M in excess of NaCl and the phenolic substances were partitioned into ethyl acetate. The ethyl acetate was evaporated and the residues resuspended in 1 mL of 50% (v/v) methanol in water. Absorbance was measured between 200 and 400 nm to estimate total phenolics per mg cell wall. The phenolic substances were separated by reverse-phase HPLC in a gradient of 1.5% (v/v) acetic acid in water to 35% acetonitrile (v/v) in 1.5% acetic acid in water (v/v), and FA and *p*CA were quantified by UV absorbance based on standards treated similarly (Hemm et al., 2003).

Pyrolysis-mass spectrometry is a rapid analytical technique to determine plant cell wall composition (Ralph and Hatfield, 1991; Vermerris and Boon, 2001). Pyrolysis-mass spectrometry analyses of stem and leaf tissue from wild-type and *bk2* cell wall preparations were performed on a Varian 1200 mass spectrometer (Varian) equipped with a PC-3 direct exposure probe (SIS). Between 5 and 10 μg of cell wall material in methanol was applied to a platinum filament and air dried. The sample was pyrolyzed inside the ion source of the mass spectrometer by resistive heating of the filament with a current of 0.5 amp at about 500°C. The pyrolysate was ionized using electron impact ionization at 70 eV, and the mass spectrometer was operated at 1,200 V. The mass range was scanned from m/z 50 to 350 with a cycle time of 0.199 s. Samples were analyzed in triplicate. The data were collected and analyzed using Varian WorkStation software.

Determination of Noncellulosic Sugars

Samples of isolated cell walls (approximately 0.5–1 mg) were hydrolyzed with 2 M TFA containing 400 nmol of myoinositol as internal standard for 90 min at 120°C in 1-mL conical Reacti-vials (Pierce Chemical). The cellulose and other undigested polymers were pelleted by centrifugation. This material was suspended in water and assayed for Glc equivalents by phenol-sulfuric colorimetric assay (Dubois et al., 1956). The TFA containing the soluble sugars was evaporated under a stream of air and the sugars were reduced with $NaBH_4$ and converted to alditol acetates as described previously (Gibeaut and Carpita, 1991). The alditol acetates were separated by gas-liquid chromatography on a 0.25-mm × 30-m vitreous silica capillary column of SP-2330 (Supelco). Temperature was held at 80°C for 1 min upon injection then programmed from 80°C to 170°C at 25°C per min, then to 240°C at 5°C per min, with a 6-min hold at the upper temperature. Monosaccharide identity, as pentose, hexose, and deoxysugar, was confirmed by electron-impact mass spectrometry (Carpita and Shea, 1989). Equimolar standards were also converted to alditol acetates to calculate response factors for quantitation of mol% relative to the myoinositol standard.

FTIR Microspectroscopy

For FTIR microscopy, approximately 5 μL of a slurry of maize cell walls from wild-type and *bk2* maize leaves and stems were spotted in individual wells of IR-reflective, gold-plated microscope slides (Thermo-Electron). The slides with cell wall samples were supported on the stage of a Continuum series microscope accessory to a 670 IR spectrophotometer with a liquid nitrogen-cooled mercury-cadmium telluride detector (Thermo-Electron). Spectra were taken in the transflectance mode, where a beam is transmitted through the wall sample, reflected off the gold-plated slide, and then is transmitted through the sample a second time before detection. One hundred twenty-eight scans were coadded at 8 cm^{-1} resolution. Each set of 10 independent samples was spotted at least five times, with a minimum of five spectra taken from isolated primary cell walls in each spot from different areas of the sample. The resulting spectra were then analyzed with WIN-DAS software (Kemsley, 1998).

Sequence data from this article can be found in the GenBank/EMBL data libraries under accession numbers AY328909 (rice *BC1* cDNA), DQ139874 (maize *Bk2* cDNA), and AL391144 (Arabidopsis *COBL4*).

ACKNOWLEDGMENTS

We thank Javier Campos for his assistance with the Klason lignin determinations, and Jason Stout, in the laboratory of Clint Chapple, for determinations of the hydroxycinnamic acids by HPLC. This is journal article number 2007–18194 of the Purdue Agricultural Experiment Station.

Received May 19, 2007; accepted October 1, 2007; published October 11, 2007.

LITERATURE CITED

Borner GHH, Lilley KS, Stevens TJ, Dupree P (2003) Identification of glycosylphosphatidylinositol-anchored proteins in Arabidopsis: a proteomic and genomic analysis. Plant Physiol **132:** 568–577

Brown DM, Zeef LAH, Ellis J, Goodacre R, Turner SR (2005) Identification of novel genes in Arabidopsis involved in secondary cell wall formation using expression profiling and reverse genetics. Plant Cell **17:** 2281–2295

Burk DH, Ye ZH (2002) Alteration of oriented deposition of cellulose microfibrils by mutation of a katanin-like microtubule-severing protein. Plant Cell **14:** 2145–2160

Carpita NC (1996) Structure and biogenesis of the cell walls of grasses. Annu Rev Plant Physiol Plant Mol Biol **47:** 445–476

Carpita NC, Defernez M, Findlay K, Wells B, Shoue DA, Catchpole G, Wilson RH, McCann MC (2001) Cell wall architecture of the elongating maize coleoptile. Plant Physiol **127:** 551–565

Carpita NC, Gibeaut DM (1993) Structural models of primary cell walls in flowering plants: consistency of molecular structure with the physical properties of the walls during growth. Plant J **3:** 1–30

Carpita NC, Shea EM (1989) Linkage structure of carbohydrates by gas chromatography mass spectrometry (GC-MS) of partially methylated alditol acetates. *In* CJ Biermann, GD McGinnis, eds, Analysis of Carbohydrates by GLC and MS. CRC Press, Boca Raton, FL, pp 157–216

Ching A, Dhugga KS, Appenzeller L, Meeley R, Bourett TM, Howard RJ, Rafalski A (2006) *Brittle stalk2* encodes a putative glycosylphosphatidylinositol-anchored protein that affects mechanical strength of maize tissues by altering the composition and structure of secondary cell walls. Planta **224:** 1174–1184

Dubois M, Gilles KA, Hamilton JK, Rebers PA, Smith F (1956) Colorimetric method for the determination of sugars and related substances. Anal Chem **28:** 350–356

Gibeaut DM, Carpita NC (1991) Tracing the biosynthesis of the cell wall in intact cells and plants: selective turnover and alteration of cytoplasmic and cell wall polysaccharides of proso millet cells in liquid culture and *Zea mays* seedlings. Plant Physiol **97:** 551–561

Hatfield RD, Jung HG, Ralph J, Buxton DR, Weimer PJ (1994) A comparison of the insoluble residues produced by the Klason lignin and acid detergent lignin procedures. J Sci Food Agric **65:** 51–58

Hauser MT, Morikami A, Benfey PN (1995) Conditional root expansion mutants of Arabidopsis. Development **121:** 1237–1252

Hemm MR, Ruegger MO, Chapple C (2003) The Arabidopsis *ref2* mutant is defective in the gene encoding CYP83A1 and shows both phenylpropanoid and glucosinolate phenotypes. Plant Cell **15:** 179–194

Iiyama K, Lam TB-T, Stone BA (1994) Co-valent cross-links in the cell wall. Plant Physiol **104:** 315–320

Kemsley EK (1998) Discriminant Analysis of Spectroscopic Data. John Wiley and Sons, Chichester, UK

Kokubo A, Kuraishi S, Sakurai N (1989) Culm strength of barley—correlation among maximum bending stress, cell wall dimensions, and cellulose content. Plant Physiol **91:** 876–882

Kokubo A, Sakurai N, Kuraishi S, Takeda K (1991) Culm brittleness of barley (*Hordeum vulgare* L.) mutants is caused by smaller number of cellulose molecules in cell wall. Plant Physiol **97:** 509–514

Lagrimini LM, Burkhart W, Moyer M, Rothstein S (1987) Molecular cloning of complementary DNA encoding the lignin-forming peroxi-

dase from tobacco: molecular analysis and tissue-specific expression. Proc Natl Acad Sci USA **84:** 7542–7546

Lane DR, Wiedemeier A, Peng LC, Höfte H, Vernhettes S, Desprez T, Hocart CH, Birch RJ, Baskin TI, Burn JE, et al (2001) Temperature-sensitive alleles of *RSW2* link the KORRIGAN endo-1,4-β-glucanase to cellulose synthesis and cytokinesis in Arabidopsis. Plant Physiol **126:** 278–288

Langham DG (1940) *Brittle stalk-2* (*bk2*). Maize Genet Coop News Lett **14:** 21–22

Lauter N, Kampani A, Carlson S, Goebel M, Moose SP (2005) microRNA172 down-regulates *glossy15* to promote vegetative phase change in maize. Proc Natl Acad Sci USA **102:** 9412–9417

Leuchter R, Wolf K, Zimmermann M (1998) Isolation of an *Arabidopsis* cDNA complementing a *Schizosaccharomyces pombe* mutant deficient in phytochelatin synthesis. Plant Physiol **117:** 1526

Li YH, Qian O, Zhou YH, Yan MX, Sun L, Zhang M, Fu ZM, Wang YH, Han B, Pang XM, et al (2003) *BRITTLE CULM1*, which encodes a COBRA-like protein, affects the mechanical properties of rice plants. Plant Cell **15:** 2020–2031

Liang CY, Marchessault RH (1959) Infrared spectra of crystalline polysaccharides. II. Native celluloses in the region from 640 to 1700 cm^{-1}. J Polym Sci [B] **39:** 269–278

Linder M, Teeri T (1997) The roles and function of cellulose-binding domains. J Biotechnol **57:** 15–28

Marita JM, Vermerris W, Ralph J, Hatfield RD (2003) Variations in the cell wall composition of maize *brown-midrib* mutants. J Agric Food Chem **51:** 1313–1321

Martin SW, Glover BJ, Davies JM (2005) Lipid microdomains—plant membranes get organized. Trends Plant Sci **10:** 263–265

May BP, Liu H, Vollbrecht E, Senior L, Rabinowicz PD, Roh D, Pan X, Stein L, Freeling M, Alexander D, et al (2003) Maize-targeted mutagenesis: a knockout resource for maize. Proc Natl Acad Sci USA **100:** 11541–11546

McCann MC, Roberts K (1991) Architecture of the primary cell wall. *In* CW Lloyd, ed, Cytoskeletal Basis of Plant Growth and Form. Academic Press, New York, pp 109–129

Moose SP, Sisco PH (1994) *Glossy15* controls the epidermal juvenile-to-adult phase transition in maize. Plant Cell **6:** 1343–1355

Multani DS, Briggs SP, Chamberlin MA, Blakeslee JJ, Murphy AS, Johal GS (2003) Loss of an MDR transporter in compact stalks of maize *br2* and sorghum *dw3* mutants. Science **302:** 81–84

Nair RB, Bastress KL, Ruegger MO, Denault JW, Chapple C (2004) The *Arabidopsis thaliana REDUCED EPIDERMAL FLUORESCENCE1* gene encodes an aldehyde dehydrogenase involved in ferulic acid and sinapic acid biosynthesis. Plant Cell **16:** 544–554

Nicol F, His I, Jauneau A, Vernhettes S, Canut H, Höfte H (1998) A plasma membrane-bound putative endo-1,4-β-D-glucanase is required for normal wall assembly and cell elongation in Arabidopsis. EMBO J **17:** 5563–5576

Pagant S, Bichet A, Sugimoto K, Lerouxel O, Desprez T, McCann M, Lerouge P, Vernhettes S, Höfte H (2002) *KOBITO1* encodes a novel plasma membrane protein necessary for normal synthesis of cellulose during cell expansion in *Arabidopsis*. Plant Cell **14:** 2001–2013

Ralph J, Hatfield RD (1991) Pyrolysis-GC-MS characterization of forage materials. J Agric Food Chem **39:** 1426–1437

Ralph J, Hatfield RD, Quideau S, Helm RF, Grabber JH, Jung H-JG (1994) Pathway of *p*-coumaric acid incorporation into maize lignin as revealed by NMR. J Am Chem Soc **116:** 9448–9456

Roudier F, Fernandez AG, Fujita M, Himmelspach R, Borner GHH, Schindelman G, Song S, Baskin TI, Dupree P, Wasteneys GO, et al (2005) COBRA, an *Arabidopsis* extracellular glycosyl-phosphatidyl inositol-anchored protein, specifically controls highly anisotropic expansion through its involvement in cellulose microfibril orientation. Plant Cell **17:** 1749–1763

Roudier F, Schindelman G, DeSalle R, Benfey PN (2002) The COBRA family of putative GPI-anchored proteins in Arabidopsis: a new fellowship in expansion. Plant Physiol **130:** 538–548

Schindelman G, Morikami A, Jung J, Baskin TI, Carpita NC, Derbyshire P, McCann MC, Benfey PN (2001) COBRA encodes a putative GPI-anchored protein, which is polarly localized and necessary for oriented cell expansion in Arabidopsis. Genes Dev **15:** 1115–1127

Sedbrook JC, Carroll KL, Hung KF, Masson PH, Somerville CR (2002) The Arabidopsis SKU5 gene encodes an extracellular glycosyl phosphatidyl-inositol-anchored glycoprotein involved in directional root growth. Plant Cell **14:** 1635–1648

Séné CFB, McCann MC, Wilson RH, Grinter R (1994) FT-Raman and FT-infrared spectroscopy: an investigation of five higher plant cell walls and their components. Plant Physiol **106:** 1623–1633

Shedletzky E, Shmuel M, Trainin T, Kalman S, Delmer D (1992) Cell wall structure in cells adapted to growth on the cellulose-synthesis inhibitor 2,6-dichlorobenzonitrile. Plant Physiol **100:** 120–130

Shi H, Kim YS, Guo Y, Stevenson B, Zhu JR (2003) The *Arabidopsis SOS5* locus encodes a putative cell surface adhesion protein and is required for normal cell expansion. Plant Cell **15:** 19–32

Simpson PJ, Xie H, Bolam DN, Gilbert HJ, Williamson MP (2000) The structural basis for the ligand specificity of family 2 carbohydrate-binding modules. J Biol Chem **275:** 41137–41142

Theander O, Westerlund EA (1986) Studies on dietary fiber. 3. Improved procedures for analysis of dietary fiber. J Agric Food Chem **34:** 330–336

Timoshenko S, Young DH (1962) Elements of Strength of Materials, Ed 4. D. Van Nostrand Company, Princeton

Tsuboi M (1957) Infrared spectrum and crystal structure of cellulose. J Polym Sci [B] **25:** 159–171

Turner SR, Taylor N, Jones L (2001) Mutations of the secondary cell wall. Plant Mol Biol **47:** 209–219

Udenfriend S, Kodukula K (1995a) How glycosylphosphatidylinositol-anchored membrane proteins are made. Annu Rev Biochem **64:** 563–591

Udenfriend S, Kodukula K (1995b) Prediction of omega site in nascent precursor of glycosylphosphatidylinositol protein. Methods Enzymol **250:** 571–581

Updegraff D (1969) Semimicro determination of cellulose in biological materials. Anal Biochem **32:** 420–424

Vermerris W, Boon JJ (2001) Tissue-specific patterns of lignification are disturbed in the *brown midrib2* mutant of maize (*Zea mays* L.). J Agric Food Chem **49:** 721–728

Wang Z, Ni Z, Wu H, Nie X, Sun Q (2006) Heterosis in root development and differential gene expression between hybrids and their parental inbreds in wheat (Triticum aestivum L.). Theor Appl Genet **113:** 1283–1294

Yong W, O'Malley R, Link B, Binder B, Bleecker A, Koch KE, McCann MC, McCarty DR, Patterson S, Reiter W-D, et al (2005) Plant cell wall genomics. Planta **221:** 747–751

Youl JJ, Bacic A, Oxley D (1998) Arabinogalactan-proteins from *Nicotiana alata* and *Pyrus communis* contain glycosylphosphatidylinositol membrane anchors. Proc Natl Acad Sci USA **95:** 7921–7926